

Thermal melting of magnetic stripe domains

W. Kuch* and K. Fukumoto†

Freie Universität Berlin, Institut für Experimentalphysik, Arnimallee 14, 14195 Berlin, Germany

J. Wang‡

Max-Planck-Institut für Mikrostrukturphysik, Weinberg 2, 06120 Halle, Germany

F. Nolting, C. Quitmann, and T. Rasmvik§

Swiss Light Source, Paul Scherrer Institute, Villigen, Switzerland

(Received 13 October 2010; revised manuscript received 3 January 2011; published 27 May 2011)

We present a microscopic investigation of the temperature dependence of stripe domains in perpendicularly magnetized Ni films on Cu(001) using photoelectron emission microscopy in combination with x-ray magnetic circular dichroism (XMCD) in the resonant absorption of soft x rays. When the temperature approaches the Curie temperature of the system, the average width of the observed stripe domains is reduced along with the XMCD contrast. In addition, the domains become mobile. A quantitative analysis of the temperature-dependent motion of the domains yields an exponential behavior of the domain mobility with temperature, pointing toward thermally activated processes.

DOI: [10.1103/PhysRevB.83.172406](https://doi.org/10.1103/PhysRevB.83.172406)

PACS number(s): 75.70.Kw, 68.37.-d, 75.70.Ak

Magnetic thin films with an out-of-plane magnetic anisotropy exhibit a typical stripe-like domain pattern, which results from the competition between exchange and Coulomb interactions.^{1,2} The appearance of domains lowers the magnetostatic demagnetizing energy on the cost of creating domain walls. The stripe domain phase shows up as characteristically inclined sections in magnetization reversal curves of perpendicularly magnetized films. Systems exhibiting the stripe domain phase at remanence are ideal for investigations that need a two-dimensional magnetic system with domains of a certain average size, such as magnetic scattering experiments,^{3,4} measurements of domain wall magnetoresistance,^{5,6} or investigations of the anomalous Hall effect.⁷ Controlling magnetic domains may play a crucial role in storing or processing magnetic information in future devices.^{8,9}

The principle of competing interactions at different length scales, which is on the basis of the occurrence of stripe domains, is quite general and, besides to magnetic stripe domains in perpendicularly magnetized systems, applies also, for example, to the charge stripe formation in doped Mott insulators¹⁰ and the pattern formation of polymers in solution or of amphiphiles in water-oil mixtures.^{11,12} Various theoretical papers deal with the nature of the ground configuration, in particular, the connection between the stripe width and magnetic properties such as exchange energy and magnetic anisotropy.^{13–17} Experimental studies have mainly focused on the appearance, size, and shape of stripe domains.^{18–24} The stripe width can be tuned most easily by controlling the magnetic anisotropy. It reduces toward the spin reorientation transition to the in-plane magnetization direction, when the effective anisotropy crosses zero.

Much less investigated are the dynamical properties of stripe domains, and their behavior upon approaching the ordering temperature of the system. On the theoretical side, Schmalian and Wolynes describe stripe domains in uniformly frustrated systems by a glass-like behavior.²⁵ In their theory, the appearance of stripe domains is explained

by a self-generated glass transition due to the emergence of an exponentially large number of metastable states. It predicts the appearance of fluctuating stripes below a transition temperature T_A , with an exponential temperature dependence of the relaxation time. The relaxation time diverges to infinity at a temperature $T_K < T_A$, the temperature at which the configurational entropy vanishes.²⁵

Portmann *et al.* were the first to report an experimental observation of a fluctuation of stripe domains.²⁶ In images of perpendicularly magnetized Fe films on Cu(001) taken with scanning electron microscopy with polarization analysis (SEMPA), they observed a characteristic ruggedness of the stripe domains indicating a movement of the stripes during the scanning acquisition of an image. This motion occurred only in a narrow temperature interval close to the ferromagnetic-paramagnetic phase transition. A quantification of this motion from the SEMPA images was not possible.

Fluctuating stripe domains would also provide an alternative explanation for an apparently paramagnetic phase close to the spin reorientation transition in Fe/Ni/Cu(001) reported by Won *et al.*²⁷ In photoelectron emission microscopy (PEEM) images the magnetic contrast vanished close to the transition from perpendicularly magnetized stripe domains to a magnetization in the film plane as a function of Fe layer thickness, which had been interpreted as a reduction of the Curie temperature at the length scale crossover from the anisotropy-dominated to the dipole-dominated regime.²⁷ The vanishing of the magnetic contrast was observed only if the temperature of the measurement was close to the Curie temperature, such that it might as well result from a mobility of stripe domains close to the Curie temperature.

Here, we present a temperature-dependent magnetic domain imaging study of ultrathin Ni films on Cu(001) which exhibit a perpendicular magnetization.^{28,29} We use PEEM in combination with x-ray magnetic circular dichroism (XMCD) in soft x-ray absorption as a magnetic contrast mechanism for the microscopic laterally resolved detection of the x-ray

absorption cross section, as described in Refs. 30–32. In PEEM, full-field images of the sample are acquired from the emitted secondary electrons by an imaging electron optics. From a series of images taken while slowly increasing the temperature of the sample, we observe and quantitatively analyze the motion of the stripe domains when approaching the Curie temperature. We find an exponential increase in the number of domain wall displacements per time interval as a function of temperature. This is consistent with a thermally activated transition between several states close in energy, as they should be present in a self-generated glass transition.

The experiments were performed at the surface and interface microscopy (SIM) beamline of the Swiss Light Source^{33,34} *in situ* in an ultrahigh vacuum system with a base pressure of 10^{-8} Pa. The disk-shaped Cu(001) single crystal was cleaned by cycles of 1 keV argon ion bombardment at 300 K and subsequent annealing at 873 K for 15 min. A commercially available PEEM (Elmitec) (Ref. 35) was used with imaging parameters set to result in a lateral resolution of 150 nm, and a field of view of $100\ \mu\text{m}$. To accelerate the image acquisition, binning of camera pixels was performed such that one pixel corresponded to 200 nm on the sample.

The Ni film was grown in the PEEM measurement position by thermal evaporation on the clean substrate at room temperature. About nine atomic monolayers (MLs) of Ni were evaporated by electron bombardment of a high purity wire (99.99% purity) of 2 mm diameter and reached the sample under an angle of 16° . During the deposition, the pressure in the chamber was kept below 5×10^{-8} Pa. The evaporation rate was around 0.5 ML/min.

Radiation from a helical undulator delivered circularly polarized radiation with a degree of polarization of $>98\%$. The exciting x rays were incident at an angle of 16° with respect to the sample surface. The XMCD images presented in the following are grayscale-coded absorption images at the Ni L_3 absorption maximum (853 eV) for positive helicity, normalized to a background image recorded at room temperature in the pre-edge region at 5 eV lower photon energy.

During the temperature-dependent measurements, the sample was constantly heated by the filament of the electron bombardment heating of the Elmitec sample holder underneath the sample using a current of 1.2 A. The temperature was monitored using a thermocouple mounted inside the sample holder. Image acquisition started 35 min after switching on the heating filament. After that time, thermal drift of the sample holder had slowed down sufficiently, and the heating rate was roughly constant at about 0.33 K/min. The exposure time per image was 32 s, subsequent images were taken every 60 s.

Figure 1 shows on the left-hand side some representative domain images during the heating. Panels (a), (c), and (e) correspond to images recorded 50, 85, and 90 min after starting the heating, respectively. Typical stripe domains are seen in (a), which are partly pinned at two scratches on the surface. In image (c), taken at about 11.6 K higher temperature at the same spot of the sample, the average stripe width as well as the domain contrast between bright and dark domains is reduced. Furthermore, both vary over the height of the image, where it is clear that the domains at the very top of the image are smaller than in the bottom part. We attribute this variation across the image to a thickness gradient of the film, due to

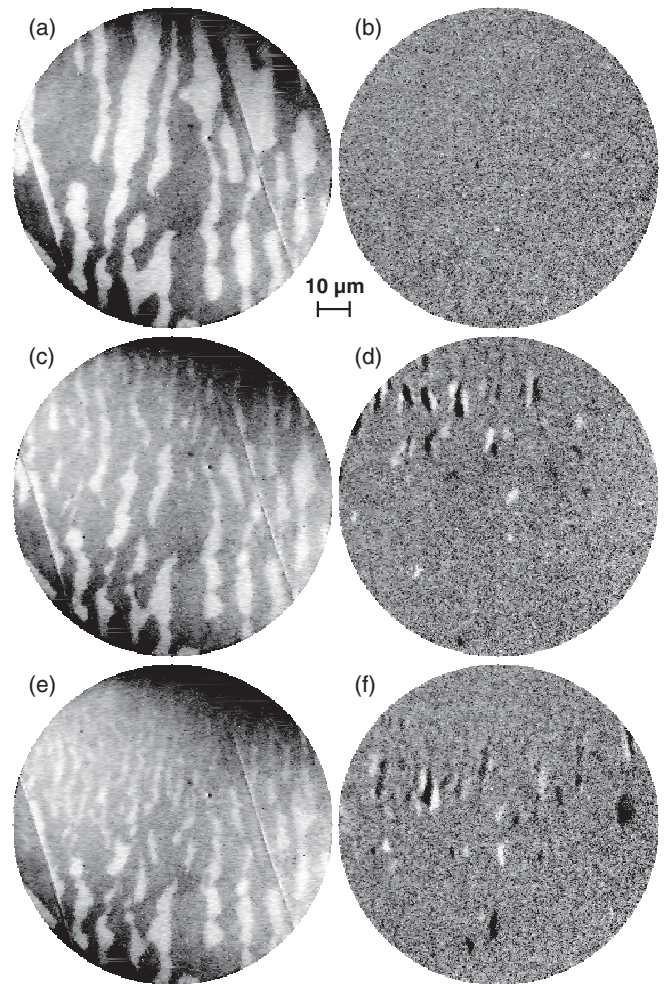


FIG. 1. (Left) Magnetic domain images of Ni/Cu(001) at different times during heating of the sample, (a) 50 min, (c) 85 min, and (e) 90 min after switching on the heating power. Images (b), (d), and (f) show the difference between the images presented in panels (a), (c), and (e), respectively, and corresponding domain images acquired 1 min later. The field of view is $100\ \mu\text{m}$.

the grazing incidence of the film deposition and possibly also some misalignment of the evaporator and/or shading by the objective lens during deposition. The Curie temperature of ultrathin Ni films on Cu(001) depends on the film thickness due to finite size scaling.³⁶ From that temperature dependence, we estimate the thickness variation as 0.3 ML across the field of view. Images presented here have been rotated such that the film thickness increases from top to bottom. The slight disparity between areas covered by dark and white domains has to be explained by the residual magnetic stray field of the objective lens of the PEEM, and possibly of the underlying heating filament. A movie showing the complete series of images is available as supplementary material.³⁷

Panel (e) in Fig. 1 shows an image taken after another 5 min, i.e., at about 1.7 K higher temperature than image (c). No more domain contrast is now observed at the top edge of the image, which at the time scale of the exposure time of 32 s appears nonmagnetic. Again it is clearly observed how the domain size, averaged over dark and bright domains,

decreases toward the top of the image, i.e., toward lower film thickness, where the film is closer to the Curie temperature at the given sample temperature. Compared to panels (a) and (c), it becomes obvious how some of the stripe domains have split into several narrower stripes. A similar reduction in domain size with temperature has been observed in Fe/Cu(001).²⁶

At the same time when shrinking in size, the domains acquire some mobility. When the domain images are viewed as a movie,³⁷ the smaller domains at the top are moving around, giving a flame-like impression. To visualize this domain mobility, difference images between the images presented on the left-hand side of Fig. 1 and the corresponding images acquired 1 min later have been calculated and are shown on the right-hand side of the figure. Black-and-white features correspond to a movement of a stripe domain, whereas purely black or white spots indicate the growing or shrinking of domains. Panel (b) does not show any such domain movements, while in panels (d) and (f) an enhanced domain mobility in the region of the smaller domains becomes evident.

For further analysis, the effect of the thickness gradient has to be excluded. This can be done by introducing the reduced temperature $T_R = T/T_C$, where T_C is the thickness-dependent Curie temperature of the film.^{38,39} To assign reduced temperature values to each sample position in each image, we first count the number of domain movements in horizontal line profiles of all the difference images such as the ones shown on the right-hand side of Fig. 1. The vertical position of the line profile with the highest number of domain displacements is then moving constantly downward toward higher thicknesses with increasing temperature. We now assume that this line corresponds to the same reduced temperature in each image, and that the variation of T_C over an image can be approximated by a linear dependence on position. T_C as deduced from the disappearance of the magnetic contrast in the images varies from about 420 K at the top of the images to about 430 K at the bottom. Plots of the number of domain displacements in the horizontal line profiles vs their vertical position for each image look similar and can be brought to overlap if they are shifted by the constant amount of 13.2 pixels or 2.6 μm for each subsequent image. By shifting all images accordingly, we obtain an approximately linear relation between the vertical position in the images, the time, and the reduced temperature, which allows us to average linescans from several images for the analysis in order to obtain a better statistics. All line profiles that correspond to the same reduced temperature are grouped together, and the average number of domain displacements in two successive images, i.e., in 1 min, is evaluated. The relative deviation in the reduced temperature of two images which are rigidly shifted is always smaller than 10^{-3} .

The result of this analysis is shown in Fig. 2 as a function of “local” time on the sample, where 2000 s correspond to the reduced temperature at which the maximum domain mobility is observed. A time span of 2000 s on the x axis corresponds to a variation of about 11 K in absolute temperature, or 0.026 in reduced temperature. The number of domain displacements first increases toward its maximum as a function of position, time, or temperature, then abruptly decreases. This decrease corresponds to the disappearance of magnetic contrast in the images, and has to be attributed to a wiping out of the domain movements by the exposure time

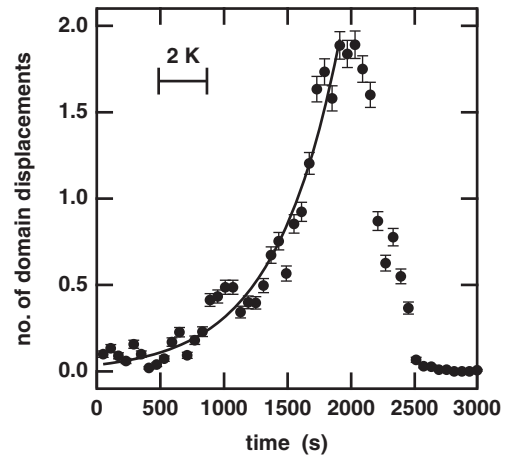


FIG. 2. Statistical evaluation of the average number of domain displacements in 1 min along a single horizontal line profile as a function of time. The x axis can be assumed to be proportional to the temperature of the sample (see text). Linescans at different positions of the image have been shifted in time according to their position relative to the disappearance of the domain pattern. The continuous line is an exponential fit to the data in the range from 0 to 1850 s. The scale bar represents the heating rate of 5.5 mK/s. The reduced temperature is defined as unity at the disappearance of the magnetic contrast, which is at about 2500 s in the graph.

of 32 s. The temperature of 420–430 K at which the XMCD contrast disappears is about 20–30 K lower than the Curie temperature reported in the literature for a Ni film of 9 ML thickness,³⁶ which is within the uncertainty of the temperature measurement.

The increase in domain mobility with temperature exhibits an exponential behavior. This is demonstrated by the solid line in Fig. 2, which is the result of an exponential fit to the data in the range of 0–1850 s. Such an exponential behavior of the stripe mobility, or inversely, of the domain relaxation time proves that we are witnessing a thermally activated process. This is consistent with the picture of thermally activated fluctuations between a large number of states with similar energy, such as in the theory of Schmalian and Wolynes.²⁵ The relevant energy barrier between two different stripe patterns has to be related to the pinning of domain walls at crystal imperfections. As soon as the thermal energy of the system exceeded the pinning energy, the domains would be constantly fluctuating in a liquid-like manner; this would correspond to the transition between a stripe glass and a stripe liquid phase.

The mobility of the stripe domains leads to the observed glass-like melting of the stripe domain pattern at a temperature below T_C . The apparent melting temperature depends on the time scale of the measurement as well as its lateral resolution. This is relevant, for example, when discussing T_C of stripe domain systems. Most techniques cannot distinguish a stripe liquid phase from the loss of long-range magnetic order at T_C . One way to do so could be the analysis of intensity correlation functions for nonergodic systems^{40,41} in resonant coherent x-ray scattering experiments taking advantage of the short pulses of a free-electron laser.⁴²

In conclusion, we have presented a microscopic PEEM investigation of the temperature dependence of stripe domains in perpendicularly magnetized Ni films on Cu(001). Besides a narrowing of the average stripe width, we also observe a thermal melting of the magnetic stripe domain pattern when approaching the Curie temperature. The mobility of the domains thereby follows an exponential behavior, which indicates thermally activated processes. This is consistent with

a glass-like behavior of the stripes below a stripe glass to stripe liquid phase transition.

We thank the Max Planck Institute of Microstructure Physics (J. Kirschner) for financial support. This work was performed at the Swiss Light Source, Paul Scherrer Institut, Villigen Switzerland.

*kuch@physik.fu-berlin.de; URL: <http://www.physik.fu-berlin.de/~ag-kuch>

†Present address: Tokyo Institute of Technology, Ookayama, Meguro-ku, Tokyo, Japan.

‡Present address: State Key Laboratory for Magnetism, Institute of Physics, Chinese Academy of Science, Beijing 100190, People's Republic of China.

§Present address: Tandbergs Patentkontor, Tordenskiolds gate 6B, 0160 Oslo, Norway.

¹A. Hubert and R. Schäfer, *Magnetic Domains* (Springer, Berlin, 2000).

²C. Kittel, *Phys. Rev.* **70**, 965 (1946).

³H. A. Dürr, E. Dudzik, S. S. Dhesi, J. B. Goedkoop, G. van der Laan, M. Belakhovsky, C. Mocuta, A. Marty, and Y. Samson, *Science* **284**, 2166 (1999).

⁴S. Eisebitt, J. Lüning, W. F. Schlotter, M. Lörger, O. Hellwig, W. Eberhardt, and J. Stöhr, *Nature* **432**, 885 (2004).

⁵A. D. Kent, J. Yu, U. Rüdiger, and S. S. P. Parkin, *J. Phys. Condens. Matter* **13**, R461 (2001).

⁶C. H. Marrows, *Adv. Phys.* **54**, 585 (2005).

⁷K. M. Seemann, Y. Mokrousov, A. Aziz, J. Miguel, F. Kronast, W. Kuch, M. G. Blamire, A. T. Hindmarch, B. J. Hickey, I. Souza, and C. H. Marrows, *Phys. Rev. Lett.* **104**, 076402 (2010).

⁸D. A. Allwood, G. Xiong, M. D. Cooke, C. C. Faulkner, D. Atkinson, N. Vernier, and R. P. Cowburn, *Science* **296**, 2003 (2002).

⁹S. S. P. Parkin, M. Hayashi, and L. Thomas, *Science* **320**, 190 (2008).

¹⁰J. M. Tranquada, B. J. Sternlieb, J. D. Axe, Y. Nakamura, and S. Uchida, *Nature* **375**, 561 (1995).

¹¹P. G. De Gennes and C. Taupin, *J. Phys. Chem.* **86**, 2294 (1982).

¹²W. M. Gelbart and A. Ben-Shaul, *J. Phys. Chem.* **100**, 13169 (1996).

¹³Y. Yafet and E. M. Gyorgy, *Phys. Rev. B* **38**, 9145 (1988).

¹⁴B. Kaplan and G. A. Gehring, *J. Magn. Magn. Mater.* **128**, 111 (1993).

¹⁵A. Kashuba and V. L. Pokrovsky, *Phys. Rev. Lett.* **70**, 3155 (1993).

¹⁶Y. Millev, *J. Phys. Condens. Matter* **8**, 3671 (1996).

¹⁷T. Polyakova, V. Zablotskii, and A. Maziewski, *J. Magn. Magn. Mater.* **316**, e139 (2007).

¹⁸R. Allenspach, M. Stampanoni, and A. Bischof, *Phys. Rev. Lett.* **65**, 3344 (1990).

¹⁹M. Speckmann, H. P. Oepen, and H. Ibach, *Phys. Rev. Lett.* **75**, 2035 (1995).

²⁰H. P. Oepen, M. Speckmann, Y. Millev, and J. Kirschner, *Phys. Rev. B* **55**, 2752 (1997).

²¹A. Vaterlaus, C. Stamm, U. Maier, M. G. Pini, P. Politi, and D. Pescia, *Phys. Rev. Lett.* **84**, 2247 (2000).

²²O. Portmann, A. Vaterlaus, and D. Pescia, *Nature* **422**, 701 (2003).

²³W. Kuch, J. Gilles, S. S. Kang, S. Imada, S. Suga, and J. Kirschner, *Phys. Rev. B* **62**, 3824 (2000).

²⁴K. Fukumoto, H. Daimon, L. Chelaru, F. Offi, W. Kuch, and J. Kirschner, *Surf. Sci.* **514**, 151 (2002).

²⁵J. Schmalian and P. G. Wolynes, *Phys. Rev. Lett.* **85**, 836 (2000).

²⁶O. Portmann, A. Vaterlaus, and D. Pescia, *Phys. Rev. Lett.* **96**, 047212 (2006).

²⁷C. Won, Y. Z. Wu, J. Choi, W. Kim, A. Scholl, A. Doran, T. L. Owens, J. Wu, X. F. Jin, H. W. Zhao, and Z. Q. Qiu, *Phys. Rev. B* **71**, 224429 (2005).

²⁸W. L. O'Brien and B. P. Tonner, *Phys. Rev. B* **49**, 15370 (1994).

²⁹B. Schulz and K. Baberschke, *Phys. Rev. B* **50**, 13467 (1994).

³⁰J. Stöhr, Y. Wu, B. D. Hermsmeier, M. G. Samant, G. R. Harp, S. Koranda, D. Dunham, and B. P. Tonner, *Science* **259**, 658 (1993).

³¹W. Kuch, R. Frömter, J. Gilles, D. Hartmann, C. Ziethen, C. M. Schneider, G. Schönhense, W. Swiech, and J. Kirschner, *Surf. Rev. Lett.* **5**, 1241 (1998).

³²W. Kuch, L. I. Chelaru, F. Offi, M. Kotsugi, and J. Kirschner, *J. Vac. Sci. Technol. B* **20**, 2543 (2002).

³³C. Quitmann, U. Flechsig, L. Patthey, T. Schmidt, G. Ingold, M. Howells, M. Janousch, and R. Abela, *Surf. Sci.* **480**, 173 (2008).

³⁴U. Flechsig, F. Nolting, A. Fraile Rodríguez, J. Krempaský, C. Quitmann, T. Schmidt, S. Spielmann, and D. Zimoch, *AIP Conf. Proc.* **1234**, 319 (2010).

³⁵E. Bauer, *J. Phys. Condens. Matter* **13**, 11391 (2001).

³⁶F. Huang, M. T. Kief, G. J. Mankey, and R. F. Willis, *Phys. Rev. B* **49**, 3962 (1994).

³⁷See supplemental material at [<http://link.aps.org/supplemental/10.1103/PhysRevB.83.172406>] for a movie of the complete series of images taken during the heating of the sample.

³⁸R. Bergholz and U. Gradmann, *J. Magn. Magn. Mater.* **45**, 389 (1984).

³⁹M. Farle, B. Mirwald-Schulz, A. N. Anisimov, W. Platow, and K. Baberschke, *Phys. Rev. B* **55**, 3708 (1997).

⁴⁰P. Pusey and W. V. Meegen, *Physica A* **157**, 705 (1989).

⁴¹M. Kroon, G. H. Wegdam, and R. Sprik, *Phys. Rev. E* **54**, 6541 (1996).

⁴²G. Grübel, *Compt. Rend. Phys.* **9**, 668 (2008).